High Resolution Lunar Mapping

End-Term Report

Team 57

Inter IIT Tech Meet 2024

November, 2024

Abstract

This report details the research and approaches made in the project focused on achieving **High-Resolution Elemental Mapping of the Lunar Surface**. Using the data from the CLASS instrument on Chandrayaan-2, we have developed a comprehensive catalog of detected X-ray fluorescence (XRF) lines along with their corresponding elemental identifications, governed by the relevant source codes used in the analysis. Additionally, we have successfully mapped the coverage of these XRF lines onto a lunar base map, providing a spatial overview of elemental distribution across the lunar surface and different types of compositional groups have been identified from the calculated ratios. Other than that we have produced some results from the elemental abundance percentages. All the data for the lunar map is added in a single map we tried to make it interactive as well.

Contents

Chapter 1

Introduction

X-ray fluorescence (XRF) spectroscopy is a powerful analytical technique widely used determining the elemental composition of surfaces in a non-destructive manner. for the space based approach, Sun acts as the main source of X-rays and characteristic X-ray emissions generated when a material is excited by an external X-ray source. XRF allows for the precise identification and quantification of elements within a area. When the surface of an airless body is exposed to solar X-rays or cosmic rays, the atoms in the surface materials absorb energy and re-emit it as fluorescent X-rays characteristic of each element. Instruments like the Chandrayaan-2 Large Area Soft X-ray Spectrometer (CLASS) use this principle to detect elemental XRF lines and map surface compositions from orbit.

To understand the lunar formation and its geological evolution, the lunar surface composition mapping has been a measure target since the ignition of lunar exploration. Nearly 20% of lunar surface has been mapped by Apollo 15 and 16 XRF experiments by Mg/Si and Al/Si ratios. Chandrayaan-1 X-ray spectrometer (C1XS) has already determined elemental abundances of about 5% of the moon.

Launched on July 22nd, 2019 by GSLV MkIII-M1 rocket from Satish Dhawan Space Centre Sriharikota, the Chandrayaan-2 mission marked an important milestone for India's lunar exploration. [4] The Chandrayaan-2 Large Area Soft X-ray Spectrometer (CLASS) analyzes the moon's surface composition b y measuring the XRF spectra. Elements like Magnesium, Silicon, Aluminum, Calcium, Titanium, Iron and Sodium, by detecting characteristics spectral emissions. [5]

1.1 XRF Analysis

As we have said before that XRF is widely used as the elemental detection in a non-destructive way, let's have a look into the basics of the XRF analysis.
High energy X-Rays are bombarded at the target material, which absorbs the energy and ejects an inner shell electron into the upper shell, leaving a vacancy. Now electrons from higher energy shells will drop down to lower shell emitting photos with corresponding energy difference, called as characteristics secondary X-Rays. There are some measure reasons for the wide use of XRF analysis in the field of compositional observations of elements for space based programs.

- **Sensitive to Surface Composition :**
  For heavier elements starting from Sodium(Na_{11}), XRF gives a wide range of win-

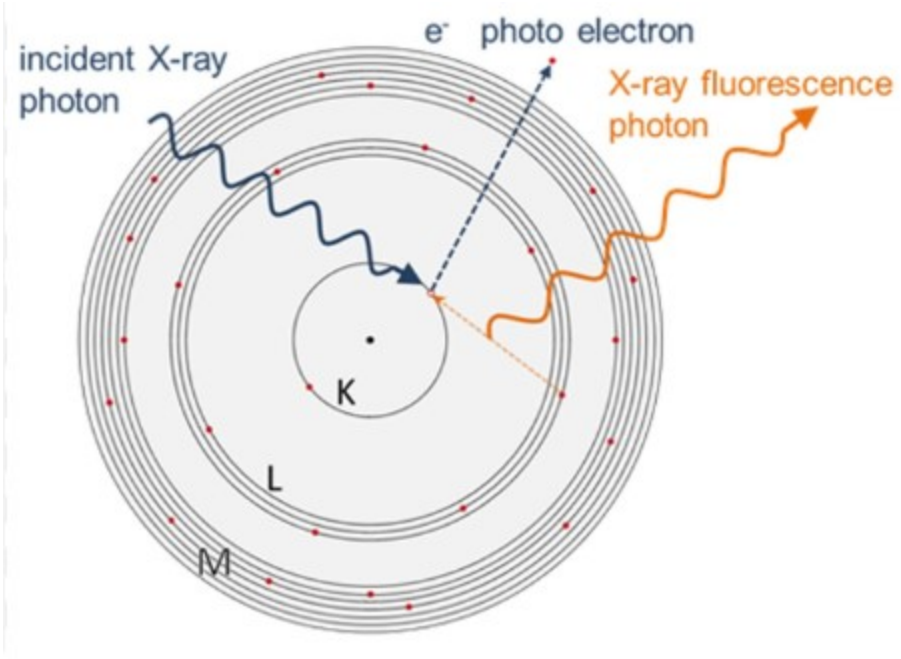

Figure 1.1: X-Ray Fluorescence Emission

dow of elemental identification. This also provides the concentration of particular elements, which is really helpful in compositional analysis.

- **Non-Destructive in Nature :**
  The procedure doesn't actually alter the structure or damage the area of sample which is required to be observed, enabling no need of on-site landing and observations. The whole surface of any celestial objects can be mapped as there is always a measure X-Ray source is present in the solar system as 'Sun'.

- **Spatial Resolution :**
  The compositional map can be created due to the availability pixel by pixel resolution from the XRF data.

1.2 The Problem Statement

As our point of interest is to make a **'High Resolution Lunar Map'** we need to make a XRF data catalog covering the useful sets of data to understand the elemental abundance in the lunar surface first. The Chandrayan-2 CLASS data should be in use. so the first task was to collect all the data and find out what are the elemental weight percentage. From the catalog itself a broader idea of elemental concentration can be visualized using a lunar base map. The XRF line coverage for the whole lunar surface by CLASS is said to be 99% and it is needed to be shown by plotting the coverage areas on a base map. From the composition percentage the possible types of rocks on the lunar surface needed to be identified.
The second part of the work mostly deals in the way to map these properties of identified areas in to the map which should be dynamic and interactive, while giving a proper quantitative idea of sub-pixel resolution.

1.3 Pre-existing Ideas About Lunar Surface

The first ever morphological idea on moon comes out when Galileo first turns his telescope towards the moon in early 1600s. The first impression on the moon was more like a separation of the dark and more brighter parts of crates and mountains. Mainly there are four theories regarding the formation of moon, the only natural satellite of mother earth. May be a bigger size planet resulting to a rotating debris, which formed moon. Probably a capture of some celestial body got trapped in the earth's gravitational field or a part broke up from earth itself. Last but not the least both the bodies might have formed at same time scale and resulted to the final structure independently.
From the early days of lunar space exploration the surface property and composition was the main point of interest for different space exploration departments.
Considering the previous Chandrayaan missions we have a very good base for the idea of elemental abundance in the lunar surface. It is well known that Oxygen is most abundant in moon surface as a part of measure rock forming mineral, where as silicon is mostly found as distributed evenly throughout the lunar surface. There is a measure co-relation between Magnesium and Aluminum can be seen. This is a fundamental property of the geochemical distribution of mafic rocks (rich in Iron and Magnesium) and Aluminum as they are produced separately and shows quite an inversion in concentration. These measure parts were found out in this particular work validating the model of working. Now as we have defined more or less basics of the XRF and lunar elemental mapping ideas let's now jump into the work and the detailed explanation of each work has been provided in the following modules.

Chapter 2

XRF-Catalog

The first part of starting the work is to gather data to play with the best approach. We have taken all the data provided by the official Pradan Website. We availed data are from 2021 to 2024 to store it and use it for our work. In the next session step by step approach has been given.

2.1 Approach

The work flow for the XRF data analysis is given below :

- **Data Extraction**
  The available fits files has a number of headers in it & are needed to be extracted first, so that a clarity of having the amount of data in our hand should be there. As suggested from the instrument basics of CLASS, it has 16 SCD (Swept charge devices) facing towards lunar surface. As we have an idea that 75% of the counts in 8s fits file comes from the area of 12.5×12.5 km, so we first have to find the area of data that is present. The 8 values of latitude and longitude gives a box structure suggesting the area traversed by a single 8s fits file by the instrument. Other than the latitude and longitude we have we have Counts and Channels present and we have to produce exactly a 2×2048 table to visualize the statistical distribution in a plot. Other header data are given in the figure.2.1

- **Data Pre-processing**
  As suggested by the user manual, the range of using XRF data is from 37 to 800, so the extra datas are needed to be cut out to get only the useful part to look at do an analysis. The channel can be converted to energy by multiplying 13.5 with the channel values.[1] So once we get the idea of the usable part of data the next part is to classify things up. Classification of data as a good fit or bad fit is extremely required as all the fits file doesn't really show up a good signal to work with. There are both flaring and non flaring regions, so according to that we need to classify the data in two parts where we say one part is a signal and the data during the non-flaring time will be the ambient noise only. Though the whole thing requires use of XSM and GOES data and we are solely using the XRF data only we have to look for a robust model of classifier that should stay strict to the instruction given. A threshold value of signal has been set and when it is matched the tested

[1] We found doing things with channel is more useful, so we didn't use the energy conversion part.

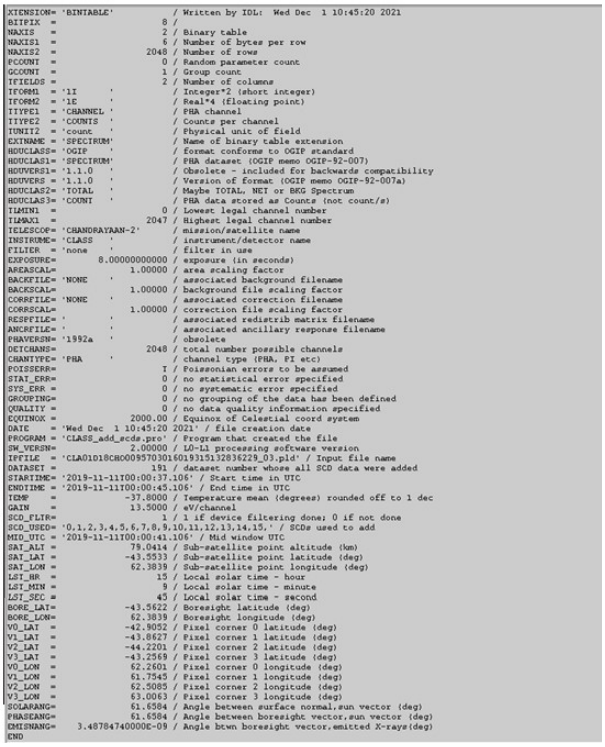

Figure 2.1: Header Data of Fits file

input fits file can be figured out as a good signal fitted file and goes into the further part of our analysis otherwise they have to go through another set of test where we have certain $2\sigma - 3\sigma$ values, to finally get the idea of that file falls into the noisy or a good fit signal category. Another approach in our work that we use by placing deterministic values of of counts range to gather the non-flaring files. A good signal data has been provided as a 2D plot in figure.2.2

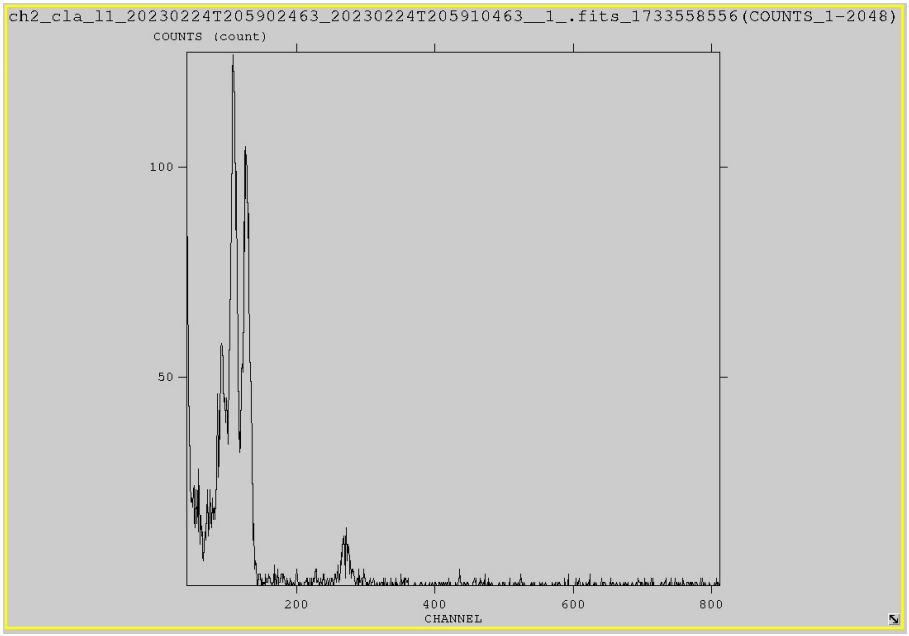

Figure 2.2: A 2D plot of COUNTS VS CHANNEL

- **Background Calculation :**

The normal idea of getting the background estimation was to identify the non-flaring times and add the fits file by time integration and to get a background estimation. But we found a rather very useful technique known as **'Moving Average Technique'**. What we actually found that these non-flaring regions sometimes contains some lone peaks which actually shouldn't be taken into analysis and we want our background estimation to be smooth and robust to give a baseline for our individual fits data. So this moving average technique helps in adapting to different fluctuations giving a more smoothened form of background noise from the non-flaring regions. The counts are averaged according to the time (8s, 16s, 32s etc.) which maintains the shape of the background after scaling things up. Unlike a static mean calculation (e.g., using an average over the entire dataset), a moving average adapts to local variations in the background. This is particularly useful in regions with slowly varying noise levels. A plot for the background estimation for individual fits file is given in the figure.

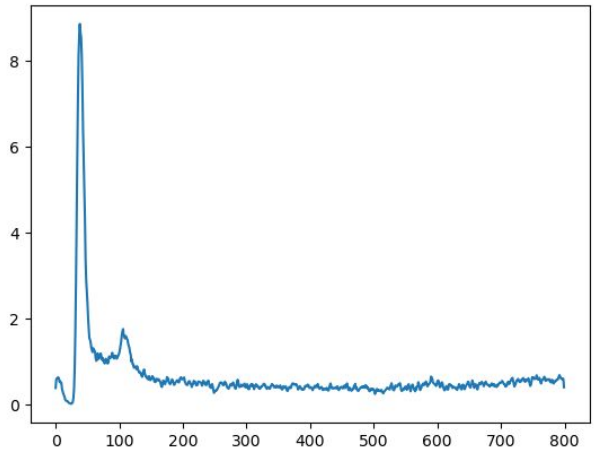

Figure 2.3: Background Estimated with moving average

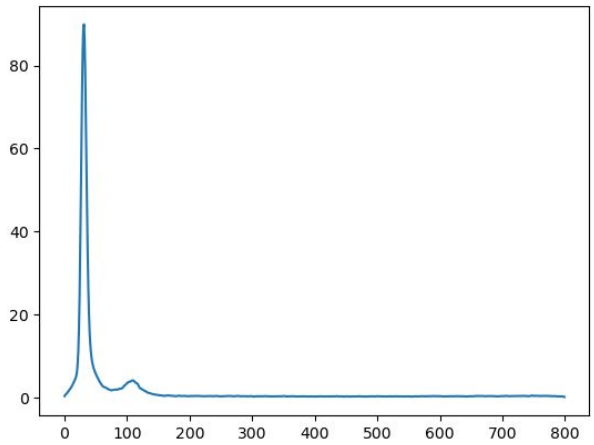

Figure 2.4: Background Smoothened

- **Gaussian Fittings :** Now as we have the background estimation for each individual 8s fits file we will now subtract the noisy things out and will try to fit gaussians to the corresponding fits plots. A general function of a gaussian is

$$y(x) = A \times exp(-\frac{(x-\mu)^2}{2\sigma^2}) \tag{2.1}$$

So we have some parameters like A, μ, σ known as amplitude, mean and standard deviation respectively. We have a number of ways we can fit these gaussian depending upon the parameter we have. So the b est thing to do was fitting all the possible gaussians and taking the best one of them into our consideration. We again need a robust classification of needed gaussian and for that some simple steps were followed. The characteristics transition lines are present on some particular channels as shown in figure. Now we make our model to fit gaussians to fit for the peaks with different masking regions. Now a dynamic gaussian selection can be done by providing different parameters for different elements. For the criteria to get the best fit gaussians, two measure ideas are imposed :

  - To keep the new gaussian fit mean closest to our characteristic mean, as the gaussian fit depends mostly upon the nearby points of the characteristics mean peak.
  - To make the area less dependent on the masking region, so that it shouldn't give a abnormal area count under it.

A plot for gaussian fits has been provided in the figure. This way of doing fittings make it completely customizable for each element

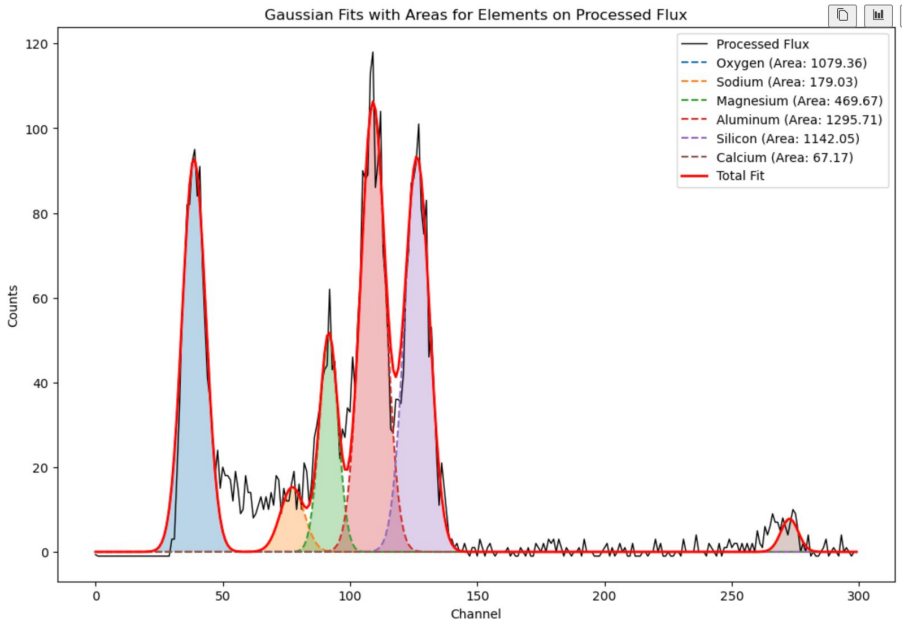

Figure 2.5: Fitted with Gaussians

- **Calculating Counts :** As we are considering the gaussian fits it is well understood that we are not picking lone standing peaks for our analysis. So now the single line peak count is not what we have, we rather have a gaussian whose area gives the net

count for the particular peak. A reason why such a approximation works is given below :

- Peak Representation: The peaks do have a gaussian shape because of the instrumental resolution corresponding any specific element.
- Total counts = Photon Flux : The area under a gaussian peak is said to be directly proportional to the emiited intensity, which is again directly relates the element's abundance after substituting a good normalizing parameter.
- Generally the area of under a gaussian peak can be given by

$$Area = A.\sigma.\sqrt{2\pi} \tag{2.2}$$

and this works as we are using regular/ gaussian peaks.

- **Overlapping Regions and Uncertainties :**
It is well observed that there is a possible overlapping between two corresponding gaussian fits, therefore a probable effective area for each gaussian fit is needed to be calculated or else an uncertainty calculation in area will give a good approximation. For that we have used the following formula :

$$\Delta A = \sqrt{(\frac{A_{overlap}}{A_1})^2 + (\frac{A_{overlap}}{A_2})^2} \tag{2.3}$$

Where $A_{overlap}$ is the overlapping are of two gaussian regions and A_1 and A_2 are two

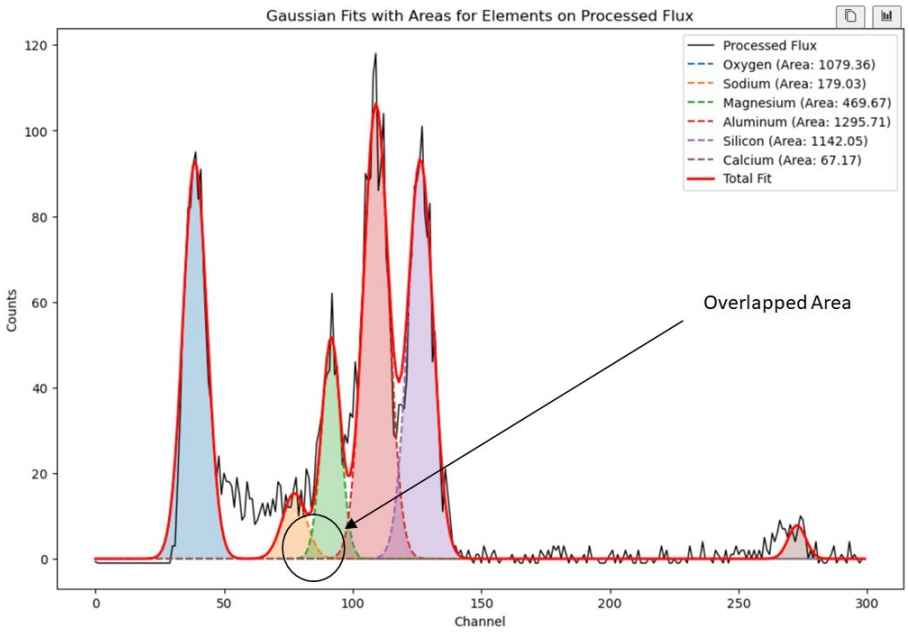

Figure 2.6: Overlapping regions

corresponding areas of two different gaussians. Again we are calculating the ratios with the silicon as silicon is the only element which is evenly distributed throughout the lunar surface. Therefore a proper calculation of uncertainty is required foe the ratio. For that case we use the formula:

$$\Delta R = R\sqrt{(\frac{A_{overlap}}{A_1})^2 + (\frac{A_{overlap}}{A_2})^2} \tag{2.4}$$

Here $R = A_1/A_2$

Once all the above written works are carried out after certain iteration[2], It's now time for to use these data and verify certain pre-existing ideas, to make a validation of our work.

2.2 XRF Line Coverage

2.2.1 Lunar Mapping the coverage of XRF lines

It is observed that the CLASS data covers almost 95% of the lunar surface but we are concerned with the particular tracks where there are solar flare events for we get good XRF line detections from these coordinates exclusively.

2.2.2 Data Collection and Initial Filtering

Downloading Files : We have downloaded all the fits file from the Pradan Website and all the fits file contains the useful coordinates of the four corners creating a box.
Parsing XML Files :

- `xml.etree.ElementTree` (referred to as xml.etree) from Python was used to parse the XML files which contains all the meta-data associated with each fits file.
- After the parsing of data is done, we were able to extract the four coordinates of the corner points for the particular region. Additionally, we have gone through the date and time information from the filenames as documented in the CH-2 user manual [7].
- Now the parsed information, including all its attributes was saved in a CSV file, which worked as a heart of the whole work, that enables a quick access to geographical and temporal information for each fits file while matching data with Solar flare data.

Filtering Based on Solar Flares:

- Using Solar Flare Database (XSM) we cross checked and took it as a reference to our fits data, which records flare events and their energy spectra over time.
- Spectrum Selection was a measure part of these works so for analysis, we looked into those events who had high energy flare flux to get a distinguishable XRF spectra which helped us in identification of elements focused on high-energy flare events, as these produce clearer and more distinguishable XRF spectra, enabling easier identification of lunar elements.

Loading the Lunar Base Map:

- We have used rasterio to load the lunar base map `(lunar_base_image.tif)` using `rasterio.open()`.
  `lunar_image = src.read(1)` This reads the base map file in 2D array.

[2]As the approach is not a straight forward one, we have implemented our unique ideas and tried to get things out with a best fitted model.

`lunar_extent = (src.bounds.left, src.bounds.right, src.bounds.bottom, src.bounds.top)` helps to capture spatial extent.
So the file is used as the base map over which we did an overlay of the XRF coverage.Map Link

2.3 Compositional Groups Based on Ratios :

Research until now suggests that lunar surface is mostly abundant with Silicon, Magnesium, Calcium, Aluminum and Titanium, but oxygen is most abundant in the minerals in the rocks. Minor elements like Sodium, Manganese, Phosphorous, Potassium were also found in very less number. According to previous studies the following minerals are majorly found on lunar crust :

Composition Group	**Description**
Pyroxene	Calcium, Iron, Magnesium Silicate compositional group.
Clinopyroxene	Pyroxene subgroup containing Calcium with a wide range of composition.
Orthopyroxene	Typically higher in Magnesium and Iron, with little Calcium.
Olivine	Magnesium-Iron Silicate compositional group.
Ilmenite	Iron-Titanium Oxide compositional group.
Feldspar	Aluminum-Silicate compositional group.
Plagioclase	Calcium-Sodium-Aluminum Silicate form of feldspar.
Anorthite	Calcium-rich plagioclase subgroup.

Table 2.1: Mineral Composition Groups and Descriptions

2.3.1 Work Flow

We have derived the percentage of different elements from the XRF data. We have used an approximate composition CSV table to match the percentage derived in the XRF analysis.

- We have defined a measuring parameter "Score" which actually defines the standard deviation in ratios.
- The score is defined as

$$\text{score} = \sqrt{\sum_i \left(\text{data\_ratio}_i - \text{group\_ratio}_i\right)^2} \tag{2.5}$$

- Lesser the standard deviation we call the particular area defined by the particular fits file will have a possibility of holding such compositional group.[3]

2.4 Challenges and Lessons Learned during the Oxygen XRF Analysis

Quite a basic idea that we got from the XRF analysis that abundance of Oxygen is the most trickier thing to find out. The reason behind it that the XRF characteristics

[3]This part was presented in the midterm submission.

of oxygen is given by it's $K\alpha$ lines which falls at the channel 37-38. There is a huge noise present all over the fits file just before 37 which influences the peak of oxygen very abruptly. While fitting gaussians most of the time we got a wrong results for which a new robust method of doing the fit analysis calculation by customizing things on the elemental basis was needed. For the sake of the elemental availability of oxygen we first analyzed the signal corresponding the peak at channel 37 and after that and then analytically mirrored the the part for the previous channels to get different masking regions. Now the same thing that we have used for the other elements is now implemented for oxygen, which produced the best fitted gaussian. From the produced gaussian we derived its photon flux and suggested that the abundance of oxygen can be derived from the XRF analysis.

Chapter 3

Elemental Lunar Base Mapping

3.1 Calculation of wt%

As discussed in the challenges we faced during the work we saw that oxygen shows a huge count. For normalizing the weight percentage Oxygen part is not considered. The sum of all photon flux has now been taken by a separate program and for each element the normalized photon flux has been found in a range of 0 to 1.[1] To make the color grading more efficient the whole value for the photon flux of each element has been normalized to 0 to 1 by it self. That means if most of the element 'X' is present in a particular area it shows more dense color as referred to the color grading.

3.2 Flowchart to Produce Base-map

The flow chart for the work has been given below :

- **Setup & Initialization:**
  - Install library `Rasterio`
  - import the library for image processing and plotting including data handling
- **Mount Drive and Read Data :**
  - Mounted Google Drive to have access to the files
  - Read the data of CSV file containing the elemental ratios and coordinates.
  - The elemental ratios are normalized to make the base map
- **Loading and Overlaying**
  - Loaded the heat map
  - Generating a heat map using `cv2`
  - Opacity and color grading has been adjusted for visualization
- **Generated Output:**
  - Different maps for different elements has been made and saved as .png extension.

[1] Can be converted in to the percentage

3.3 Results :

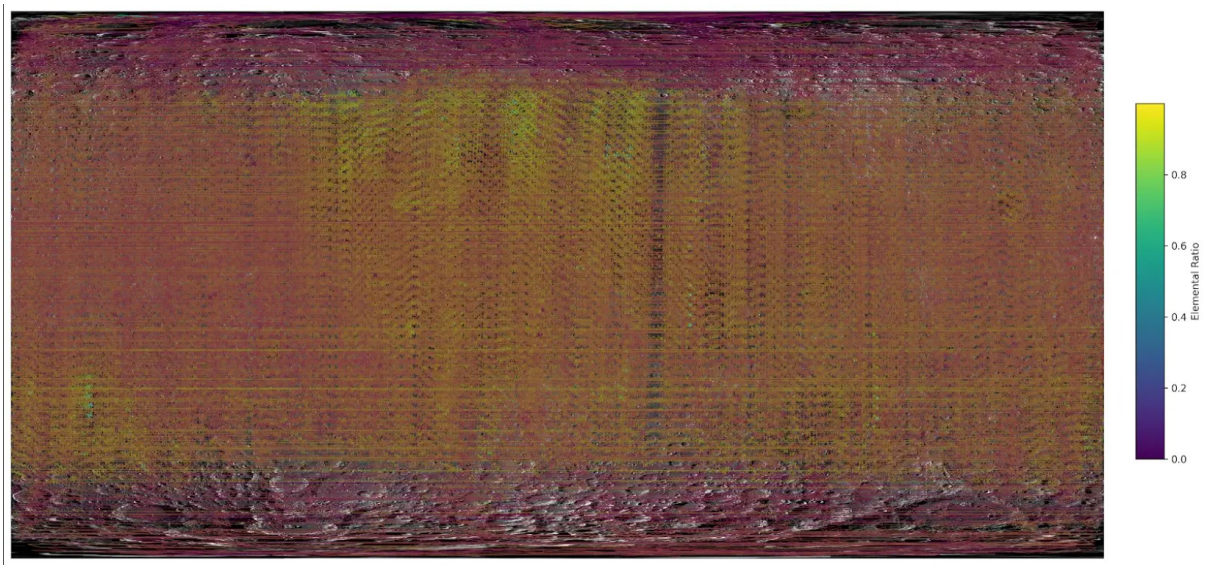

Figure 3.1: Mg Coverage map

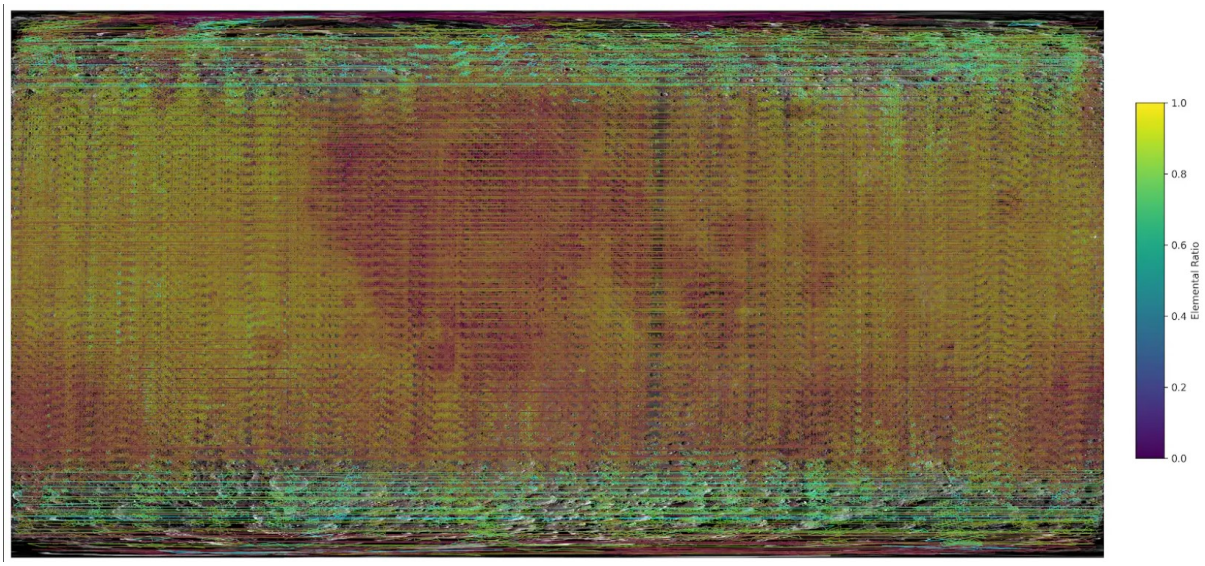

Figure 3.2: Al Coverage map

All the produced Base maps has been given in this section and valuable produced results were validated. There is a great catch in accumulation of Aluminum, Magnesium and Iron has been provided in the first part of the report. The 'mafic' elements don't really co-exist with the Aluminum and our results also satisfies that. we can see a strong co-relation between Aluminum wt% and Magnesium wt% as they show a certain inversion in the heat map.

If we concentrate on the area of **'Oceanus Procellarum'**, famously known as 'Ocean of Storms" on the lunar surface has a very rich geochemical distribution of mafic elements rather than feldspathic material (rich in Aluminum), which is a proven result suggesting

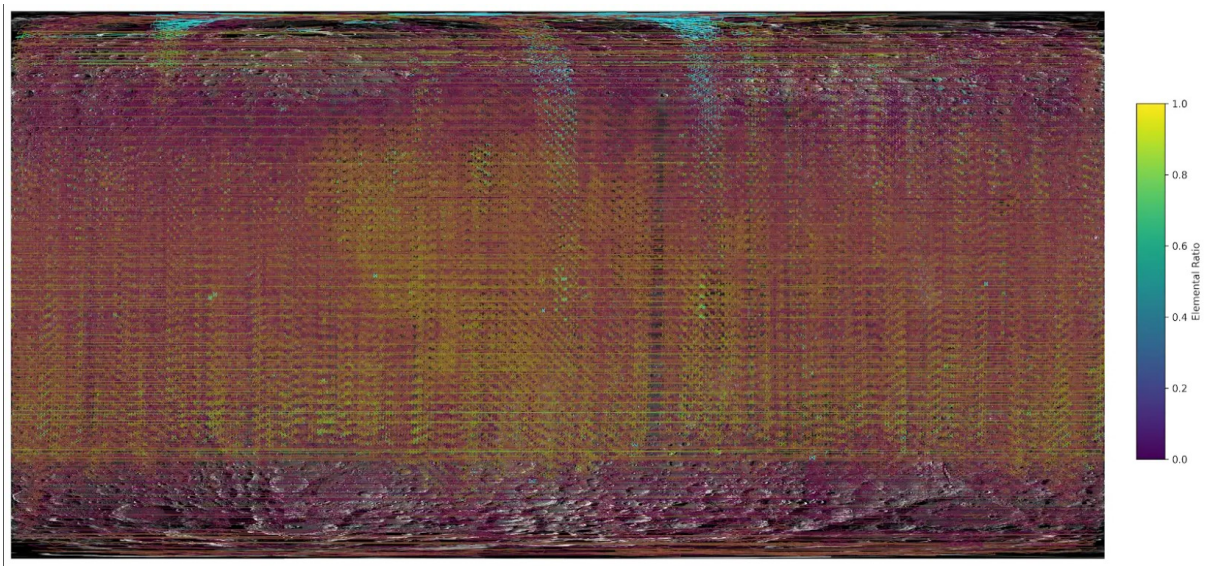

Figure 3.3: Fe Coverage Map

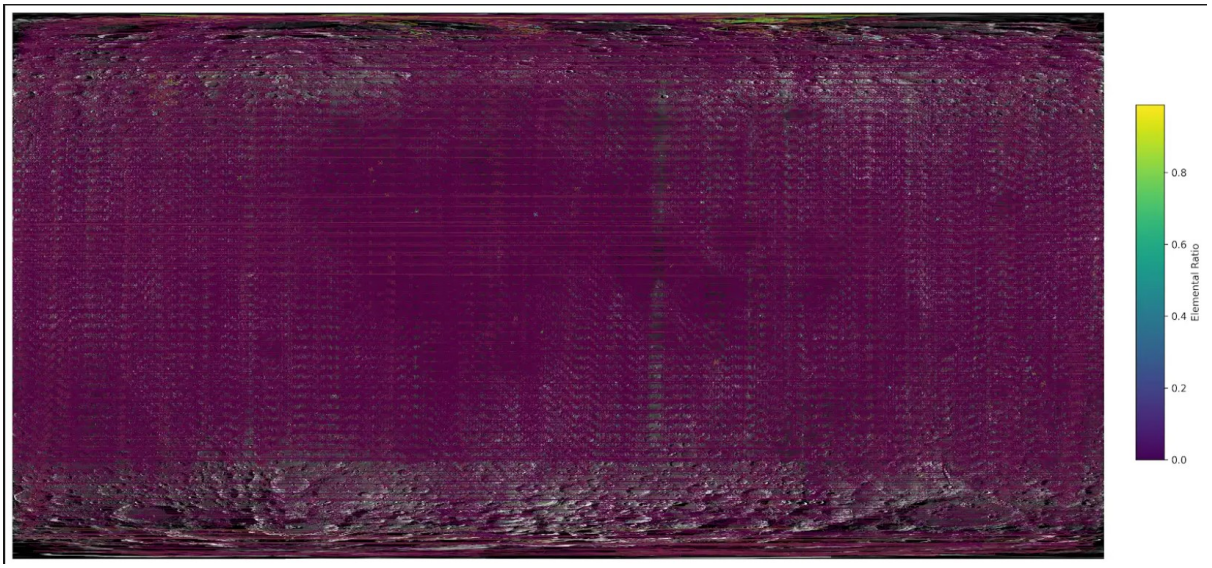

Figure 3.4: Ca Coverage map

the occurrence of higher concentration of pyroxene and olivine in these regions with a lower concentration of silica and the reason behind such a geochemical distribution in the region results due to lack of plate tectonics on lunar surface, so the mafic element generally produced in volcanic eruptions stayed there.[2]

[2]Volcanic eruptions in Oceanus Procellarum happened probably due to its thin crust.

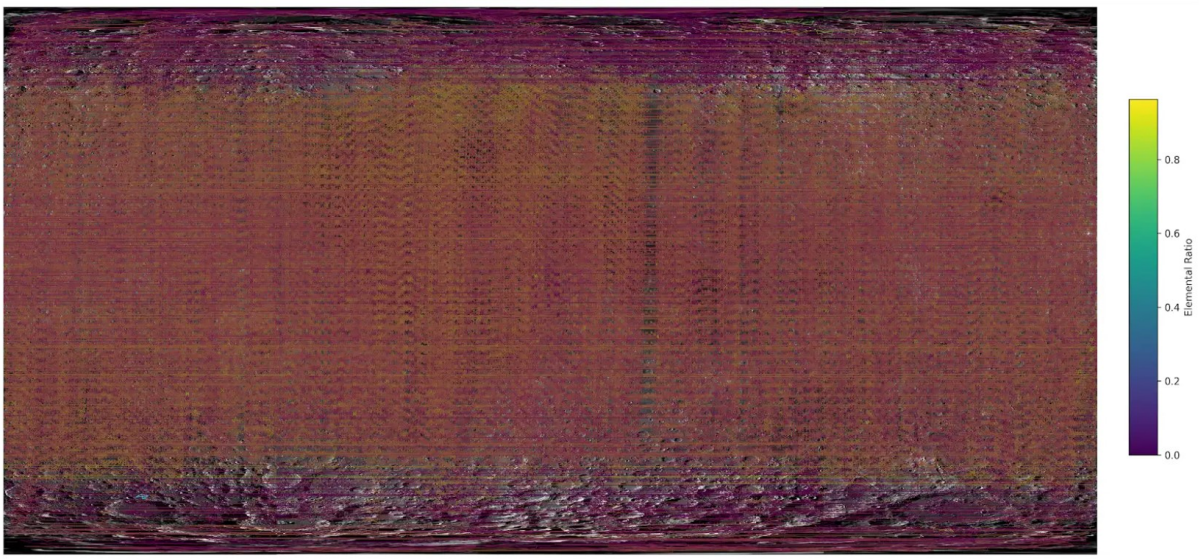

Figure 3.5: Si Coverage Map

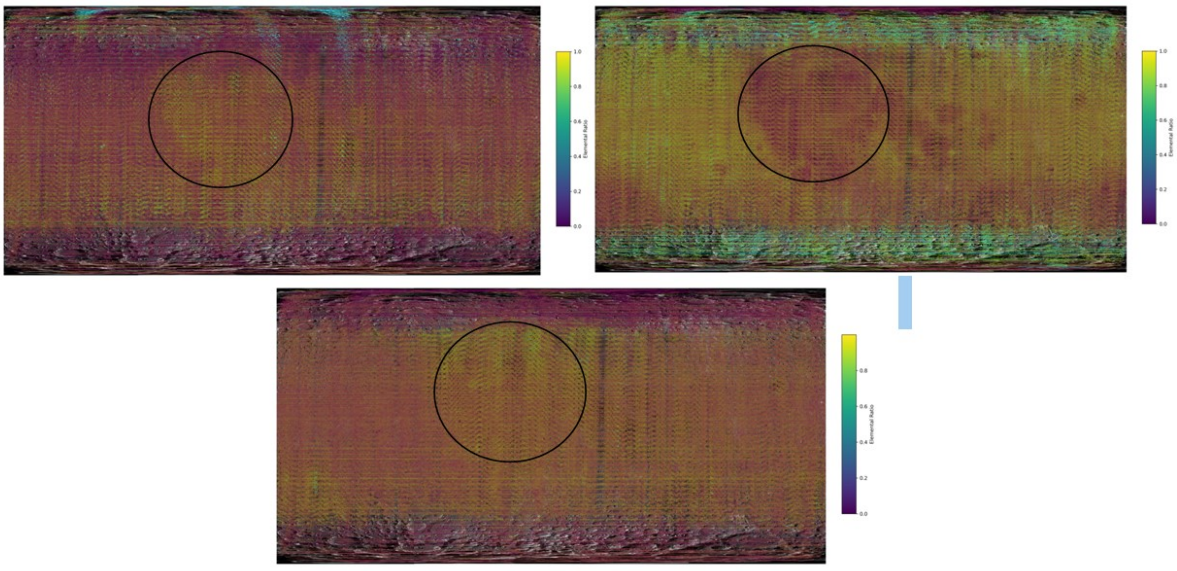

Figure 3.6: Co-relation between Fe-Al-Mg

Chapter 4

Interactive Map

So as we have a lots of data for a particular small area of $12.5km \times 12.5km$ we need all the data to be visible in an interactive map. Where each points describes the relative ratio of each element with silicon, wt% of each element as calculated. In the next session we have discussed all the libraries and scripts used to produce it.

4.1 Approach & Methodology

The whole structured code generates an interactive map of the lunar surface using a very powerful Python library **Plotly**.We have used the produced CSV file of all the data from the XRF analysis and placed it over an lunar albedo map.

- **Libraries Used :**
  - Pandas : This is used to load and manipulate the data in CSV. Again the processing the data in CSV also requires this library.
  - Numpy : Again we need many mathematical operations efficiently for that reason we will be using Numpy library
  - PIL (Python Imaging Library): We first need to open the albedo map and load kit and can be done by the 'image' module in the PIL library and the dimension of the image can also be extracted correctly as it is very much vital for the mapping of different points in the lunar base albedo map.
- **Image Optimization :**
  - WebGL Rendering: This part of the code ensures a smooth performance for a very big dataset that we have. This module will utilize the GPU for rendering, which helps to efficiently handle all the tough graphic-intensive task. `Scattergl` has been used for the smoothened performance using GPU acceleration.
  - Pixel Coordinate Mapping : We need a dynamical way of calculating the pixel co-ordinates from the given longitude and latitude as we are using these numerical values as a mapping. We need to avoid the hard-coding values and therefore the dynamical calculation of pixel co-ordinates are required.
  - Efficient Hover Data : We need the data to be retrieved without overloading the figure layout so this is where the use of Custom Hover Templates comes out, which actually retrieves data as a custom visualization.

- Aspect Ratio Preservation : The visual consistency is needed to be maintained for the whole map, there fore the aspect ratio is needed to be preserved.

4.2 Flowchart of the Interactive Map

- **Setup & Initialization:**
  - Installing libraries
  - Accessing required CSVs
  - Loading Lunar map
  - Using PIL to extract its dimension
- **Load and Validate Data:**
  - Loading CSV into `Pandas`
  - Ensuring it has all the needful data columns
- **Data Processing :**
  - Taking out the latitude longitude datas
  - Converting them into pixel coordinates
  - Aligning Pixel Coordinates with the dimension of the actual lunar base map
- **Interactive Map Creation :**
  - Used `Plotly` to create the interactive figure
  - Addition of albedo lunar map as background image
  - Efficient rendering requires `Scattergl`
  - Data points plotted on the map by `Scattergl`
  - Efficiently hovered the information
- **Customization and layout :**
  - Aspect ratio maintained
  - Axes Scaled
  - Axis labels aligned with the image
  - Marker sizes optimized
  - Marker opacity varied
  - Optimized the clarity and information
- **Generated Output:**
  - Interactive map saved as an HTML file for viewing and sharing.[1]

[1]Requires heavy RAM to view properly due to a huge dataset.

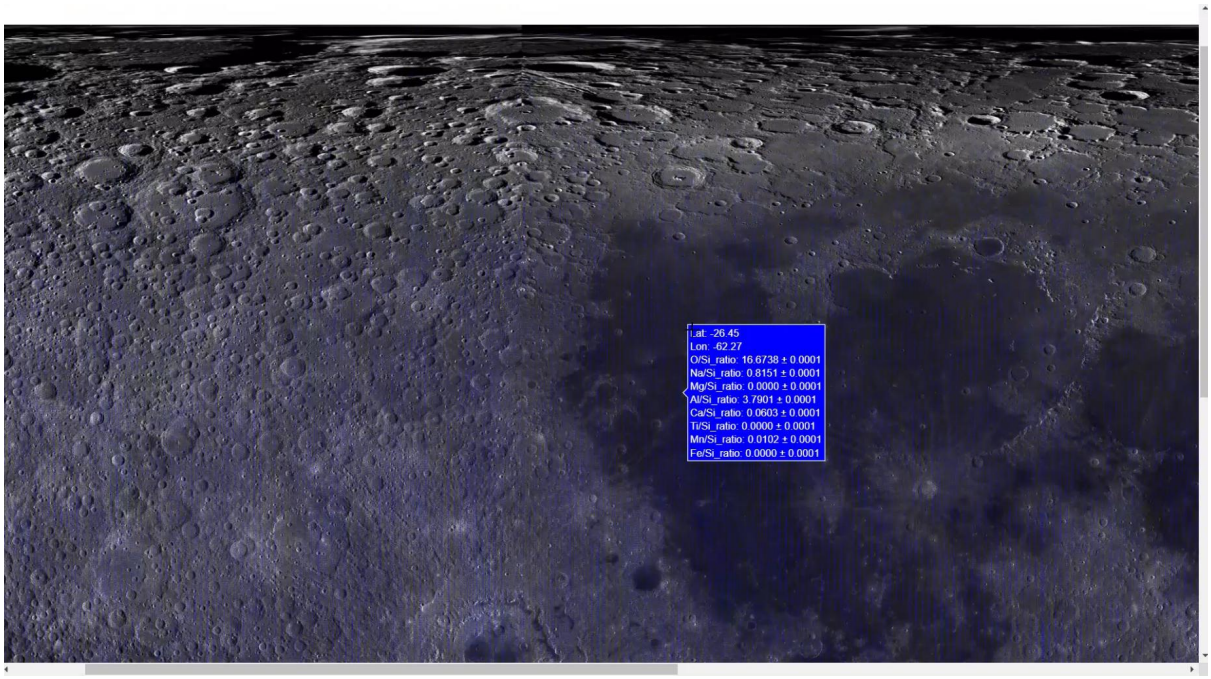

Figure 4.1: Example of our Interactive Lunar Map

4.3 Sub-Pixel Resolution : Quantitative Idea

While doing the XRF line coverage we can see lots of areas corresponds to overlaps. So the properties that we will have for the overlapped areas will get enhanced and a more accurate idea of the elemental abundance can be visualized. So while showing the interactive map we are creating two different points for the region. The property for the two different points are given by the averages. So now instead of a whole $12.5km \times 12.5km$ box property we will have more number of points due to the overlaps inside this box resulting into smaller boxes inside this core $12.5km \times 12.5km$.

Chapter 5

Future Prospects

GAN based methods have been increasingly gaining traction in the field of image analysis for super-resolution and have shown considerable improvements in image resolution [1]. In [2] the MFSR (Multi-Frame Super Resolution Method) was used to train a deep learning architecture on the LRO (Lunar Reconnaissance Orbiter) mission data for super resolution. There have also been advances in the application of deep learning networks for cosmological simulation models to achieve better resolution [3].

In the case of the CLASS lunar XRF data it will be novel and interesting to integrate a deep learning-assisted super-resolution generative adversarial network (Deep SRGAN) which could potentially help in resolving data much beyond the pixel resolution limit of the device.

Statistical learning methods used in experimental particle physics [6] are also very relevant in signal detection techniques on XRF elemental spectra. We can have coherent signal/background discrimination tasks using supervised learning to direct data-driven approaches, as we know the theoretical transition values of the elements in which we are interested.

Bibliography

[1] Chunwei Tian and Xuanyu Zhang and Jerry Chun-Wei Lin and Wangmeng Zuo and Yanning Zhang and Chia-Wen Lin. *Generative Adversarial Networks for Image Super-Resolution: A Survey*. 2022. URL: https://arxiv.org/abs/2204.13620.

[2] Delgado-Centeno, J. I. and Sanchez-Cuevas, P. J. and Martinez, C. and Olivares-Mendez, M.A. *Enhancing Lunar Reconnaissance Orbiter Images via Multi-Frame Super Resolution for Future Robotic Space Missions*. URL: https://ieeexplore.ieee.org/document/9488313.

[3] Li, Yin and Ni, Yueying and Croft, Rupert A. C. and Di Matteo, Tiziana and Bird, Simeon and Feng, Yu. *AI-assisted superresolution cosmological simulations*. 2021. URL: http://dx.doi.org/10.1073/pnas.2022038118.

[4] S. Narendranath, Netra S. Pillai, K. Vadodariya, Srikar P. Tadepalli, A. Sarwade, V. Sharan¸Radhakrishna V, A. Tyagi, M. Bhatt. *NEW LUNAR ELEMENTAL MAPS FROM CHANDRAYAAN-2*. 2023. URL: https://www.hou.usra.edu/meetings/lpsc2023/pdf/2191.pdf.

[5] S. Narendranath, Netra S. Pillai, M. Bhatt, K. Vadodariya, Radhakrishna Vatedka, Srikar P. Tadepalli, A. Sarwade, A. Tyagi, V. Sharan. *Lunar elemental abundances as derived from Chandrayaan-2*. 2024. URL: https://doi.org/10.1016/j.icarus.2023.115898.

[6] Schwartz, Matthew D. *Modern Machine Learning and Particle Physics*. 2021. URL: https://doi.org/10.48550/arXiv.2103.12226.

[7] SPACE ASTRONOMY GROUP, UR RAO SATELLITE CENTRE, ISRO. *CLASS USER MANUAL*. 2021. URL: https://pradan.issdc.gov.in/ch2/protected/downloadFile/class/ch2_class_pds_release_38_20240927.zip.